

## Preclinical Development

## Nanaomycin A Selectively Inhibits DNMT3B and Reactivates Silenced Tumor Suppressor Genes in Human Cancer Cells

Dirk Kuck<sup>1</sup>, Thomas Caulfield<sup>2</sup>, Frank Lyko<sup>1</sup>, and Jose L. Medina-Franco<sup>2</sup>

## Abstract

Enzymes involved in the epigenetic regulation of the genome represent promising starting points for therapeutic intervention by small molecules, and DNA methyltransferases (DNMT) are emerging targets for the development of a new class of cancer therapeutics. In this work, we present nanaomycin A, initially identified by a virtual screening for inhibitors against DNMT1, as a compound inducing antiproliferative effects in three different tumor cell lines originating from different tissues. Nanaomycin A treatment reduced the global methylation levels in all three cell lines and reactivated transcription of the *RASSF1A* tumor suppressor gene. In biochemical assays, nanaomycin A revealed selectivity toward DNMT3B. To the best of our knowledge, this is the first DNMT3B-selective inhibitor identified to induce genomic demethylation. Our study thus establishes the possibility of selectively inhibiting individual DNMT enzymes. *Mol Cancer Ther*; 9(11); 3015–23. ©2010 AACR.

## Introduction

The genetic information of a human cell is packaged into chromatin, which has an important biological function by controlling the accessibility of the DNA to the cellular transcription and replication machinery. Therefore, chromatin is labeled with different marks on the histones and on the DNA itself (1, 2). These marks represent the epigenetic code resulting from modification and regulation systems. The best-characterized mark on DNA consists of a single methyl group at the C5 position of cytidine nucleotides, which occurs nearly always in a CpG sequence context in differentiated cells.

The human genome encodes three active DNA methyltransferases: DNMT1, DNMT3A, and DNMT3B. DNMT1 and DNMT3B are indispensable for embryonic development in mice, whereas DNMT3A knockout mice die shortly after birth (3). DNMT1 is required for the maintenance of DNA methylation patterns during replication in normal and cancer cells and is essential for their proliferation and survival (4). DNMT3A and DNMT3B are *de novo* methyltransferases involved in embryonic devel-

opment and in the establishment of genomic imprints (3, 5, 6). The analysis of DNA methylation patterns in normal and tumor cells has revealed that many, if not all, human tumors exhibit an altered methylation signature. This aberrant methylation pattern is often characterized by hypermethylation and inactivation of tumor suppressor genes such as *p16* or *RASSF1* (7), which can consequently drive tumor formation. However, in contrast to classic genetic mutations, these so-called epimutations are reversible by the inhibition of DNMTs (8). This reversibility encouraged the development of pharmacologic inhibitors of DNA methylation.

Several approaches have been pursued to inhibit DNMT activity, including small interfering RNA-mediated depletion of DNMTs (9) or the use of suicide nucleoside substrates such as azacytidine and decitabine for covalent enzyme trapping (10). Both drugs were approved by the Food and Drug Administration for the treatment of myelodysplastic syndrome in 2004 and 2006, respectively, and represent the first DNMT inhibitors in clinical use. One of the most recent approaches is the rational development of small-molecule nonnucleoside inhibitors such as RG108 (11–13). The family of nonnucleoside candidate DNMT inhibitors is steadily growing and comprises a large variety of different chemical scaffolds [e.g., polyphenolic compounds such as epigallocatechin-3-gallate (14, 15) or compounds with acidic functions such as caffeic acid (16) or methylenedisalicylic acid (17)]. In addition, approved drugs for other indications such as hydralazine (18, 19), procaine (20, 21), procainamide (22), or antibiotics such as mithramycin A (23) have also been reported to inhibit DNA methylation. Additional DNMT inhibitors are reviewed elsewhere (10, 24, 25).

Antibiotics usually target cell wall synthesis, protein translation, or the DNA replication machinery in bacteria.

**Authors' Affiliations:** <sup>1</sup>Division of Epigenetics, German Cancer Research Center, Heidelberg, Germany and <sup>2</sup>Torrey Pines Institute for Molecular Studies, Port St. Lucie, Florida

**Note:** Supplementary material for this article is available at Molecular Cancer Therapeutics Online (<http://mct.aacrjournals.org/>).

Current address for D. Kuck: Global Drug Discovery, Research and Development, Bayer Schering Pharma, Berlin, Germany.

**Corresponding Author:** Dirk Kuck, German Cancer Research Center, Im Neuenheimer Feld 580, Heidelberg BW 69120, Germany. Phone: 49-6221-42-3807; Fax: 49-6221-42-3802. E-mail: d.kuck@dkfz-heidelberg.de

doi: 10.1158/1535-7163.MCT-10-0609

©2010 American Association for Cancer Research.

However, antibiotics of the anthracycline group, such as daunomycin, doxorubicin, or mitomycin, are also known to have powerful antitumor activity. Many related chemical structures from the anthracycline group have been developed as anticancer drugs (26, 27). Nanaomycin A also belongs to this class of quinone antibiotics isolated from a culture of *Streptomyces* (28). The nanaomycin A mode of action is dependent on its reduction by the respiratory chain-linked NADH or flavin dehydrogenase of the organism. The reduced form of nanaomycin A is quickly autooxidized by molecular oxygen producing singlet molecular oxygen ( $O_2^-$ ). The ability to produce  $O_2^-$  is related to the antimicrobial activity of nanaomycin A (29, 30). The chemical structure of nanaomycin A is depicted in Fig. 1A.

In this study, we characterized the epigenetic effects of nanaomycin A, which we had identified by an *in silico* screening approach aiming for novel inhibitors of DNMT1 (17). Nanaomycin A showed no activity against DNMT1, despite sharing structural similarities to other active compounds, such as methylenedisalicylic acid derivatives, yet we did observe a potent antiproliferative effect in different tumor cell lines. When we analyzed the genomic methylation levels in different tumor cell lines, we found a distinct nanaomycin A–dependent reduction, as well as transcriptional reactivation and expression of the *RASSF1A* tumor suppressor gene. To identify the cellular target of nanaomycin A, we applied a biochemical *in vitro* methylation assay using human DNMT1 or DNMT3B and detected a selective inhibition of DNMT3B. To better rationalize the biochemical activity at the molecular level, we conducted molecular docking studies of nanaomycin A with a homology model of DNMT3B. The docking model suggests that nanaomycin A can bind in the catalytic site of the enzyme. Currently, this is the first report of a DNMT3B-selective small-molecule inhibitor with cellular activity, highlighting the feasibility of discovering compounds that selectively inhibit individual DNMT enzymes.

## Materials and Methods

### Compounds

Nanaomycin A (NSC267461) was obtained from the National Cancer Institute (NCI)/Developmental Therapeutics Program Open Chemical Repository (<http://dtp.cancer.gov>), dissolved in DMSO to 50 mmol/L, and stored at  $-80^\circ\text{C}$ . Chemical structure of nanaomycin A is shown in Fig. 1A. 5-Azacytidine, RG108, and procainamide were purchased by Sigma-Aldrich. 5-Azacytidine and procainamide were dissolved in water; RG108 was dissolved in DMSO.

### Cell culture

A549, HL60, and HCT116 cells were obtained directly from the American Type Culture Collection and passaged in our laboratory for <6 months after resuscitation. A549, HCT116, and HeLa were cultured in DMEM/

Ham's F12 (Biocrom) supplemented with 10% FCS (Invitrogen). HL60 cells were cultured in RPMI 1640 supplemented with 5% L-glutamine and 10% FCS (Invitrogen) at  $37^\circ\text{C}$  and 5%  $\text{CO}_2$ . Determination of cell viability was done by counting the viable cells after trypan blue staining. Therefore, cells were seeded in triplicates in six-well plates at a density of 250,000 per well. Cells were treated with increasing doses of nanaomycin A for 72 hours. Caspase-3/7 activation was measured by the Caspase-Glo 3/7 assay from Promega according to the manufacturer's protocol. Cells were seeded in 96-well plates in triplicates at a density of 10,000 per well and incubated for 72 hours. Assays were measured by a Tecan Infinite 200 microplate reader.

### DNA methylation analysis

Genomic DNA was purified using the DNeasy Blood and Tissue kit (Qiagen). Global methylation levels were determined by capillary electrophoresis as described previously (31). Briefly, 5  $\mu\text{g}$  of genomic DNA were enzymatically hydrolyzed to single nucleotides, and the nucleotides were derivatized with the fluorescent marker BODIPY (Molecular Probes). Derivatized nucleotides were separated by capillary electrophoresis and analyzed in a Beckman P/ACE MDQ Molecular Characterization System. Statistical significance was calculated by the Student's *t* test.

### Methylation analysis of the *RASSF1A* promoter region

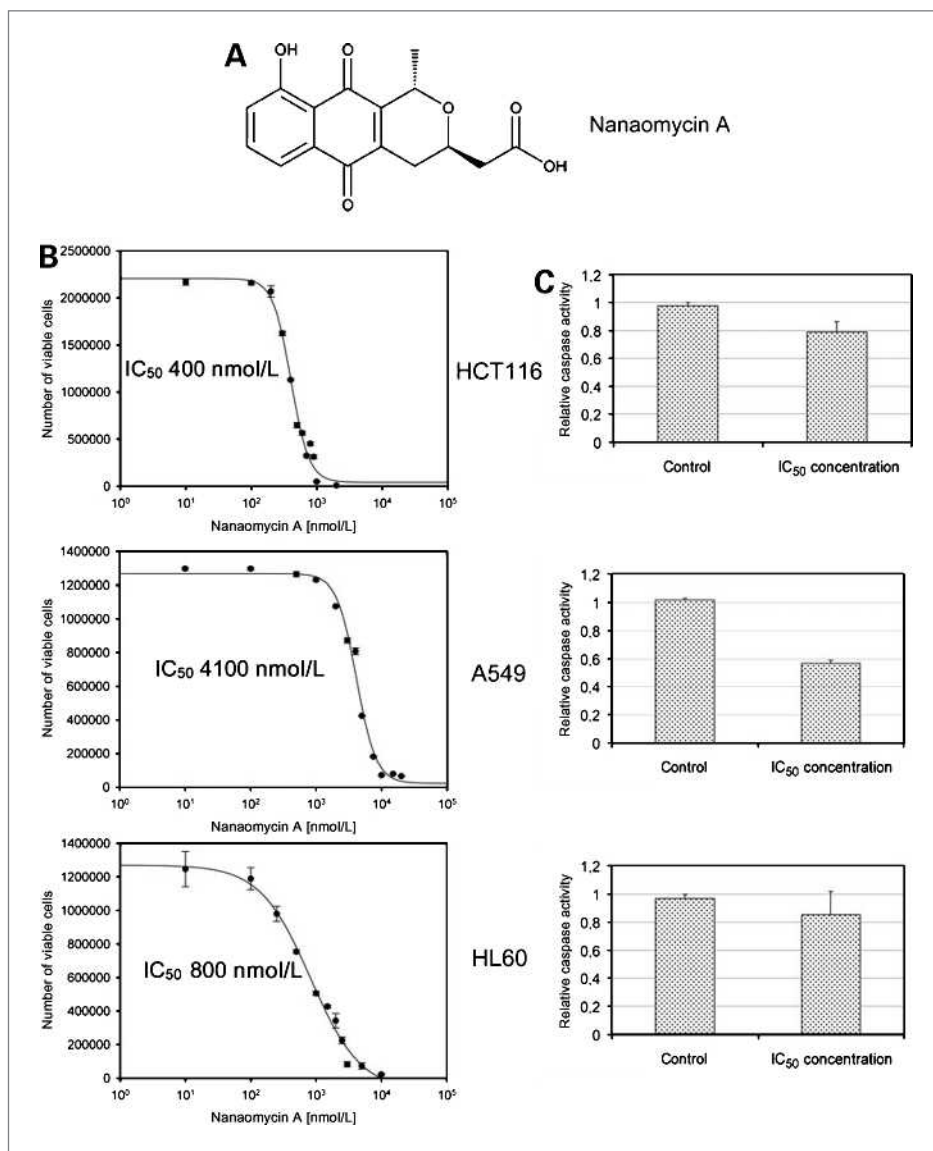
For gene-specific methylation analysis, genomic DNA was deaminated using the EpiTect Bisulfite kit (Qiagen). For 454 sequencing, bisulfite-treated genomic DNA was amplified using sequence-specific primers containing treatment-specific barcodes and 454 linker sequences: Pair1, GCCTCCCTCGCGCCATCAGTCAGGACAGTGGGGATTTTTTTTTTTTA (For\_RASSF1A\_1) and GCCTTGCCAGCCCGCTCAGTCAGGACAACAACCAATAAACTCAAAC (Rev\_RASSF1A\_1); Pair2, GCCTCCCTCGCGCCATCAGTCAGCACAGTGGGGATTTTTTTTTTTTTTTTA (For\_RASSF1A\_2) and GCCTTGCCAGCCCGCTCAGTCAGCACAACAACCAATAAACTCAAAC (Rev\_RASSF1A\_2).

PCR conditions were as follows: initial denaturation at  $95^\circ\text{C}$  for 2 minutes, 35 cycles at  $95^\circ\text{C}$  for 30 seconds, annealing at  $40^\circ\text{C}$  for 30 seconds, elongation at  $74^\circ\text{C}$  for 30 seconds, and a final elongation step at  $74^\circ\text{C}$  for 2 minutes. 454 deep sequencing was done by the German Cancer Research Center Genomics and Proteomics Core Facility.

### RNA isolation and quantitative real-time PCR

RNA was extracted using the RNeasy RNA Isolation kit (Qiagen), and on-column DNA digestion was done using the RNase-Free DNase Set (Qiagen). For quantitative reverse transcription-PCR (RT-PCR), 1  $\mu\text{g}$  of RNA was reverse transcribed using SuperScript III reverse transcriptase (Invitrogen) according to the manufacturer's protocol. Each cDNA sample was analyzed in

**Figure 1.** A, chemical structure of nanaomycin A. B, cell viability of HCT116, A549, and HL60 cell lines was determined by counting viable cells after trypan blue staining. Cells were treated with increasing doses of nanaomycin A ranging from 10 nmol/L to 10  $\mu$ mol/L for 72 h before analysis. Number of viable cells per milliliter was plotted against nanaomycin A concentrations in nmol/L. Points, mean of three wells; bars, SD. The data were analyzed by SigmaPlot version 10.0. C, activity of caspase-3 and caspase-7 in HCT116, A549, and HL60 cells was measured by Caspase-Glo 3/7 after 72 h of incubation with the calculated IC<sub>50</sub> concentrations. Results are expressed relative to those obtained in the untreated control cells. Treatment with nanaomycin A showed no induction of caspases under these conditions.



triplicate using the QuantiFast SYBR Green PCR kit (Qiagen) according to the manufacturer's instructions. QuantiTect Primer Assays (Qiagen) were used for detection of *RASSF1A*, *DNMT1*, and *DNMT3B*. *GAPDH* served as internal standard. RT-PCR was done by Light-Cycler 480 from Roche.

#### Western blot analysis

Antibodies for detection were used according to the manufacturer's protocol. The antibodies against  $\beta$ -actin, DNMT1, DNMT3B, and RASSF1A were purchased by Santa Cruz Biotechnology or by Millipore for  $\gamma$ H2AX (clone JBW301).

#### Cloning and purification of recombinant DNMTs

DNMT1 was produced and purified as described before (21). DNMT3B (isoform 2) was produced and purified

as described elsewhere (17). Briefly, proteins were expressed in insect cells and purified by affinity chromatography and gel filtration. The protein concentration of purified DNMT was determined by Bradford assay and verified by using Coomassie blue-stained SDS-polyacrylamide gels and suitable molecular mass markers of known concentration.

#### Biochemical DNMT assay

DNA methylation assays were carried out in total reaction volume of 25  $\mu$ L containing 0.4  $\mu$ mol/L hemimethylated or unmethylated oligonucleotide substrate purchased from MWG (upper strand: 5'-GATCGCX-GATGCGXGAATXGCGATXGATGCGAT-3', X = 5mC for hemimethylated or X = C for unmethylated substrate, and lower strand: 5'-ATCGCATCGATCGC-GATTCGCGCATCGGCGATC-3'), purified DNMT in

reaction buffer [100 mmol/L KCl, 10 mmol/L Tris-Cl (pH 7.5), 1 mmol/L EDTA], and bovine serum albumin (1 mg/mL). All reactions were carried out at 37°C in the presence of 0.7  $\mu$ mol/L [methyl-<sup>3</sup>H]AdoMet (2.6 TBq/mmol; Perkin-Elmer). After 3 hours, the reaction was stopped by adding 10  $\mu$ L of 20% SDS and spotting of the whole volume onto DE81 cellulose paper. Filters were baked at 80°C for 2 hours and washed three times with cold 0.2 mol/L  $\text{NH}_4\text{HCO}_3$ , three times with distilled water, and once with 100% ethanol. After drying, filters were transferred into Mini-Poly Q vial from Perkin-Elmer, and 5 mL of Ultima Gold LSC Cocktail were added per vial. Analysis was done in a scintillation counter, and each measurement was repeated once.

### Molecular docking

The structure of nanaomycin A was prepared with the program Molecular Operating Environment (MOE; version 2008.10; Chemical Computing Group, Inc.). Docking studies were conducted with Glide (version 5.5; Schrödinger, LLC), and visualizations were carried out with Maestro (version 9.0; Schrödinger, LLC). Docking was done using previously generated homology models of DNMT3B (17) and DNMT1 (32). The scoring grids were centered on the binding mode predicted for 2'-deoxycytidine as we reported previously (17). We used the bounding box size 14Å × 6Å × 10Å, which covers the catalytic pocket and part of the cofactor binding site. We used flexible docking with the extra precision mode in Glide and default parameters. To explore the putative interactions of nanaomycin A with the binding site, the top-ranked binding mode found by Glide in complex with the binding pocket of the enzyme was subjected to full-energy minimization using the MMFF94x force field implemented in MOE until a gradient of 0.001 was reached. The default parameters implemented into the LigX application of MOE were used.

### Results

In an earlier study, we conducted a virtual screening of a public compound library from the NCI using a multi-step docking approach with a previously validated homology model of the catalytic domain of human DNMT1 (17). Docking was completed using three different programs. From this, nanaomycin A (Fig. 1A, chemical structure) was ranked among the top 10% of all screened compounds from two of the docking programs. However, this quinonic compound did not show any detectable DNMT1 inhibition. When we treated three different human tumor cell lines [HCT116 (colon), A549 (lung), and HL60 (bone marrow)] with increasing concentrations of nanaomycin A (ranging from 10 nmol/L to 10  $\mu$ mol/L) for 72 hours, we observed in all three cell lines a distinct cytotoxic effect (Fig. 1B). We determined the cellular viability by counting viable cells after trypan blue staining and measured  $\text{IC}_{50}$  values of 400 nmol/L for HCT116, 4100 nmol/L for A549, and 800 nmol/L for HL60. These data suggest a broad antiproliferative activity, which does not seem to be restricted to specific cell types.

The balance between cell proliferation and cell death is regulated by apoptotic and necrotic pathways. To elucidate the cellular mechanism of nanaomycin A-dependent cell death, we measured caspase-3 and caspase-7 activities in nanaomycin A-treated cells. Therefore, cells were incubated for 72 hours with the  $\text{IC}_{50}$  concentrations. However, when we compared untreated control cells with cells treated with the calculated  $\text{IC}_{50}$  concentrations, we did not detect activation of caspase-3 and caspase-7 (Fig. 1C). Thus, we conclude that caspase activation does not play a major role in the measured cell death.

Studies from various cancers have shown that downregulation of genes by DNA methylation as well as maintenance of silencing are important mechanisms through which tumor cells can survive (7). Thus, we decided to analyze a possible interruption of these mechanisms and assessed the ability of nanaomycin A to decrease

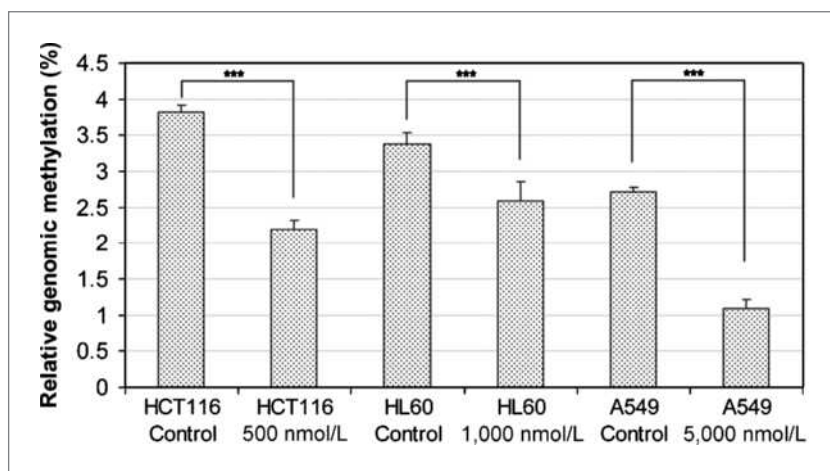
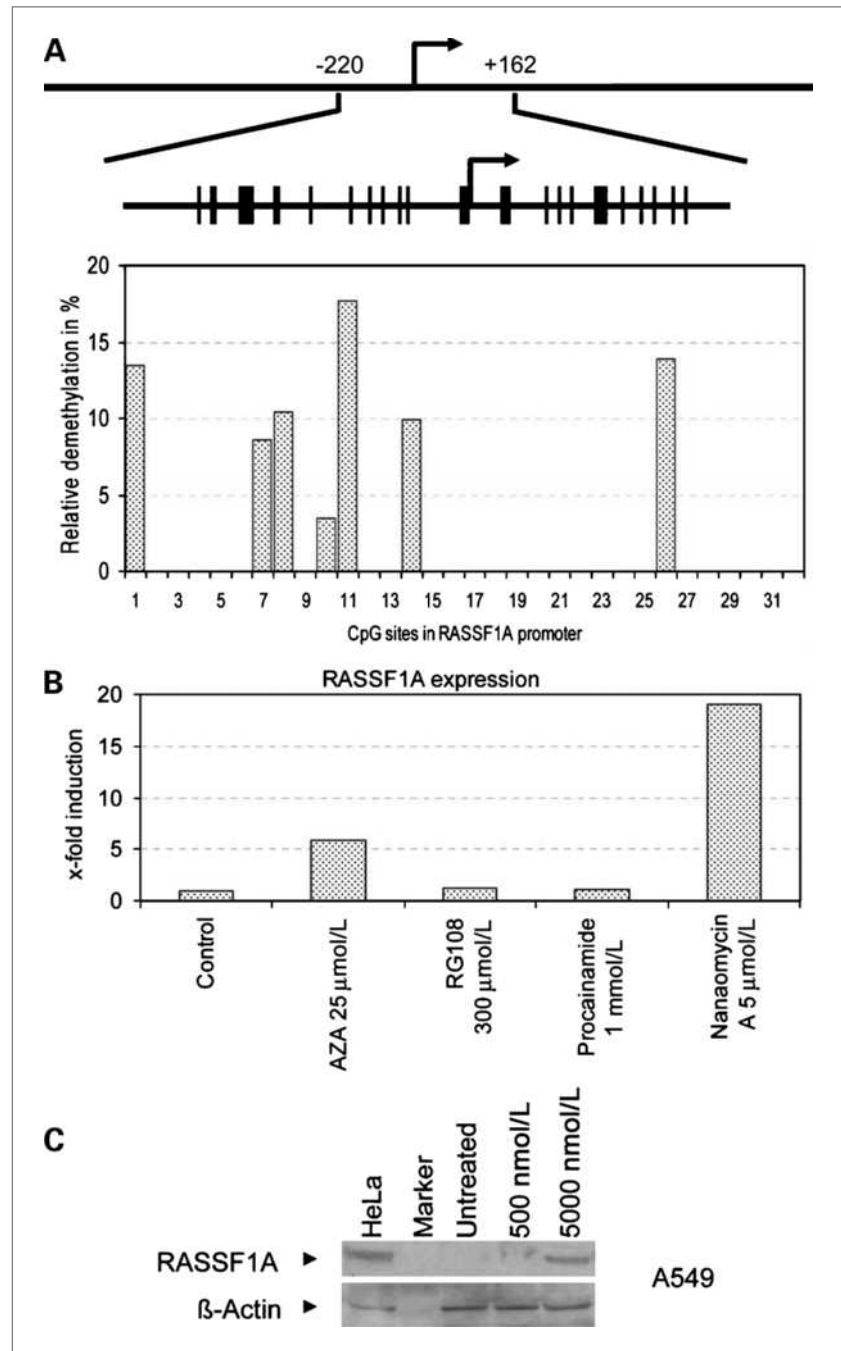


**Figure 2.** Relative genomic cytosine methylation levels in percentage of HCT116, HL60, and A549 were determined by capillary electrophoretic analysis. Cells were incubated for 72 h with the indicated nanaomycin A concentration. Bars, SD. Asterisks denote a statistically significant ( $P < 0.001$ ) difference compared with the untreated control cells. Statistical significance was calculated by the Student's *t* test. Nanaomycin A induced in all three cell lines a significant genomic demethylation compared with control cells.



**Figure 3.** A, 454 bisulfite sequencing of the *RASSF1A* promoter region in untreated and nanaomycin A–treated A549 cells. Cells were incubated for 72 h with nanaomycin A (5,000 nmol/L), genomic DNA was isolated and bisulfite treated, and the *RASSF1A* locus was amplified by PCR before sequencing. Illustrated are the relative demethylation levels in percentage of treated cells to untreated cells for 31 CpG sites within the *RASSF1A* promoter. Nanaomycin A treatment resulted in demethylation that was restricted to a few CpG sites. B, quantitative RT-PCR analysis of *RASSF1A* transcription normalized to *GAPDH* in A549 cells after treatment with 5-azacytidine (AZA; 25  $\mu$ mol/L), RG108 (300  $\mu$ mol/L), procainamide (1 mmol/L), and nanaomycin A (5,000 nmol/L) for 72 h. Points, mean of three wells; bars, SD. Nanaomycin A and 5-azacytidine were able to reactivate *RASSF1A* transcription after treatment. C, Western blot of A549 cells treated with nanaomycin A (500 and 5,000 nmol/L) for 72 h. Whole-cell lysates were assayed for expression of *RASSF1A* protein (top) and  $\beta$ -actin (bottom). Fifty micrograms of total protein were loaded for HeLa cells as positive control, and 250  $\mu$ g for A549 samples. Nanaomycin A treatment revealed induction of *RASSF1A* protein expression in A549 cells.



the genomic methylation level of HCT116, HL60, and A549 cells by capillary electrophoresis (Fig. 2; ref. 31). We incubated cells for 72 hours with 500 nmol/L for HCT116, 1,000 nmol/L for HL60, and 5,000 nmol/L for A549 and isolated genomic DNA. Genomic methylation levels were found to be most significantly ( $P < 0.001$ ) reduced in HCT116 at 500 nmol/L (from 3.8% to 2.2%), in HL60 at 1,000 nmol/L (from 3.4% to 2.6%), and in A549 at 5,000 nmol/L (from 2.7% to 1.1%). Although we used compound concentrations in the range of the calculated

$IC_{50}$  value, we measured genomic demethylation also with lower nanaomycin A concentrations (e.g., at 100 nmol/L for HL60 or at 3,000 nmol/L for A549; data not shown). This argues against the hypothesis that the observed demethylation might be a toxic side effect of the treatment. From this, we assumed that nanaomycin A hits the same cellular target in all three cell lines.

One of the primary biological outcomes of DNA methylation in cancer cells is transcriptional repression of tumor suppressor genes, thus promoting uncontrolled

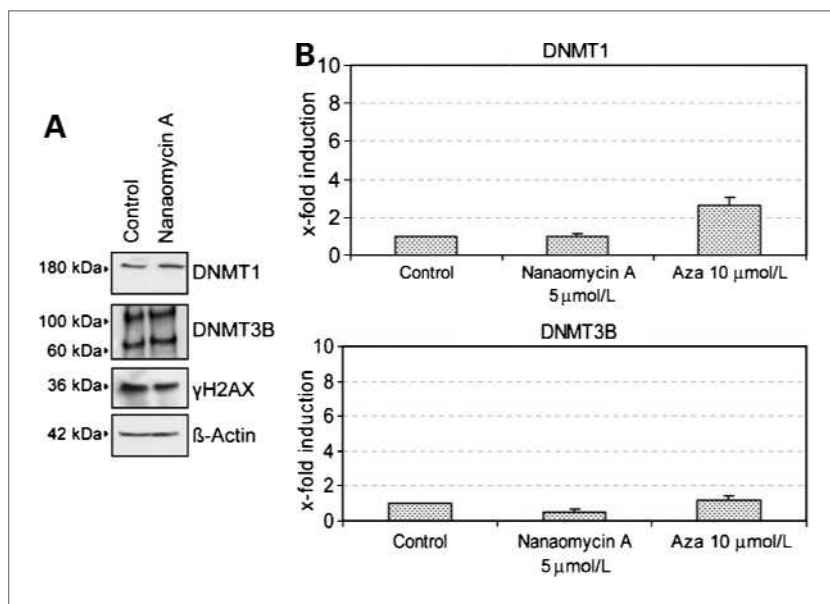


**Figure 4.** A, Western blot analysis of A549 cells untreated (control) and treated with nanaomycin A (5,000 nmol/L) for 72 h. Detection was carried out for DNMT1, DNMT3B,  $\gamma$ H2AX, and  $\beta$ -actin as loading control. Displayed are representative Western blots. Treatment of cells with nanaomycin A caused no significant changes on protein levels. B, quantitative RT-PCR analysis of *DNMT3B* or *DNMT1* expression normalized to *GAPDH* in A549 cells after treatment with nanaomycin A (5,000 nmol/L) and 5-azacytidine (Aza; 10  $\mu$ mol/L) as reference compound. Points, mean of three wells; bars, SD. Nanaomycin A induced no changes in transcript levels of *DNMT3B* or *DNMT1*.

proliferation (7). For this reason, we investigated the promoter methylation of the epigenetically silenced *RASSF1A* tumor suppressor gene in untreated and nanaomycin A-treated (5,000 nmol/L) A549 cells. We used 454 bisulfite sequencing of the *RASSF1A* promoter region with coverage rates between 450 and 600 reads per CpG (Fig. 3A). Sequencing confirmed that the *RASSF1A* promoter was heavily methylated in A549 cells. Nanaomycin A treatment resulted in demethylation that was restricted to a few CpGs, which is in line with the results obtained after DNMT3B knockdown in A549 cells (33).

We next assessed *RASSF1A* transcript levels relative to *GAPDH* transcript levels by quantitative RT-PCR after treatment with several concentrations of nanaomycin A. We used 5-azacytidine (25  $\mu$ mol/L), RG108 (300  $\mu$ mol/L), and procainamide (1 mmol/L) as reference compounds (Fig. 3B). We observed a ~6-fold relative induction after 5-azacytidine treatment and an 18-fold relative induction after treatment with nanaomycin A (5,000 nmol/L). Lower concentrations of nanaomycin A yielded lower relative *RASSF1A* induction (e.g., 3,000 nmol/L induced 2-fold induction; data not shown). Procainamide or RG108 treatments achieved no reactivation.

Parallel assessment of *RASSF1A* protein expression by Western blotting revealed an initiation of *RASSF1A* protein expression in A549 cells (Fig. 3C). HeLa extracts were used as positive control for *RASSF1A* protein expression. In conclusion, we provide evidence for genomic and locus-specific demethylation caused by nanaomycin A that is apparently sufficient to reactivate transcription and expression of a silenced tumor suppressor gene.

Because the known antimicrobial mode of action of nanaomycin A involves free radical generation, we hypothesized that nanaomycin A might directly degrade DNMT1 or DNMT3B in compound-treated cells. To ex-

perimentally test this hypothesis, we did Western blotting and quantitative RT-PCR of untreated and nanaomycin A (5,000 nmol/L)-treated A549 cells and failed to detect any evidence for DNMT protein degradation (Fig. 4A) or downregulated DNMT transcription levels (Fig. 4B). We also tested whether DNA might be damaged by nanaomycin A treatment. However, A549 cells treated with nanaomycin A did not show increased levels of the DNA damage marker  $\gamma$ H2AX by Western blot analysis (Fig. 4A). These experiments strongly suggest that nanaomycin A does not directly degrade DNMT1 or DNMT3B in compound-treated cells.

After analyzing indirect inhibition of DNMTs, we investigated the possibility of direct inhibition of DNMTs by nanaomycin A. We focused on DNMT1 and DNMT3B, the two most important isoforms in tumorigenesis, using a biochemical *in vitro* methylation assay consisting of recombinant methyltransferases. Human methyltransferases DNMT1 and DNMT3B were produced via baculovirus-mediated expression in SF9 insect cells and purified by affinity chromatography and gel filtration (21). Strikingly, we found a pronounced selectivity of nanaomycin A toward DNMT3B in the tested compound range with an  $IC_{50}$  value of 500 nmol/L (Fig. 5A). Under these conditions, the enzymatic activity of DNMT1 was not affected by nanaomycin A. To our knowledge, this is the first report of a non-SAH (S-adenosyl-L-homocysteine) analogue acting as a DNMT3B-selective inhibitor (34, 35).

To explore the putative binding mode of nanaomycin A with DNMT3B, we applied molecular docking of the inhibitor with a homology model of the catalytic site of DNMT3B (17). To build our computational model, the homology model of DNMT3B was constructed with Prime (Schrödinger, LLC) using the crystal structure of DNMT3A (PDB code 2QRV) as a template (36). The final

homology model showed a backbone root mean square deviation of only 0.08 Å with the template; further details are published elsewhere (17). Figure 5B shows the optimized binding model of nanaomycin A with DNMT3B. According to this binding model, residues that form the binding pocket of nanaomycin A include Pro<sup>650</sup>, the catalytic Cys<sup>651</sup>, Glu<sup>697</sup>, Arg<sup>731</sup>, Arg<sup>733</sup>, Lys<sup>828</sup>, Gly<sup>831</sup>, and Arg<sup>832</sup>. The carboxylic acid group of the ligand is capable of forming hydrogen bonds with the side chain of Arg<sup>832</sup>. Notably, with nanaomycin A, both the hydroxyl group and adjacent carbonyl oxygen atom are predicted to form an extensive hydrogen bond network with the side chains of Arg<sup>731</sup> and Arg<sup>733</sup>. Additionally, the hydroxyl group of the ligand forms a hydrogen bond with the side chain of Glu<sup>697</sup>. Interestingly, we do not observe similar hydrogen bonds with the equivalent glutamic acid and arginine residues in docking studies of nanaomycin A with a previously validated homology model for the catalytic site of human DNMT1 (32), which provides a possible structural explanation for the enzyme selectivity of the drug.

## Discussion

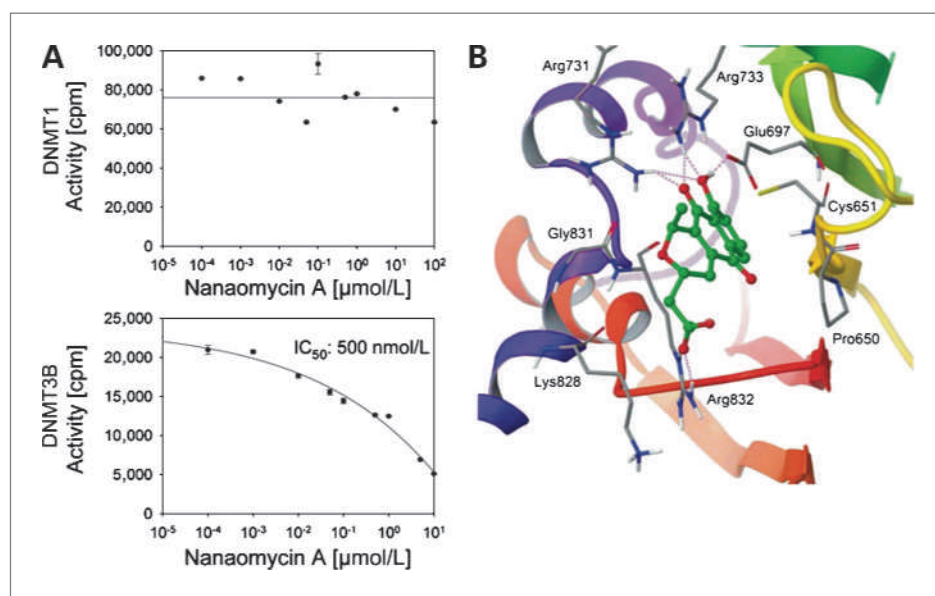
The number of compounds reported to possess DNA demethylating properties without covalent binding is steadily growing. Due to the high conservation of the catalytic domain within the DNMT family, most compounds are not expected to show selectivity to individual DNMT enzymes. Additionally, many of these compounds revealed weaker inhibition potential when compared with nucleoside analogues (37). Treatment of MCF-7 cells with procaine reduced the genomic methylation level ~40% and reactivated transcription of the tumor suppressor gene *RARβ2*, although the demethylation around the

transcription start site was moderate (20). Procainamide treatment of HCT116 cells also induced global demethylation by ~15% and a similar degree of locus-specific demethylation at the *TIMP3* tumor suppressor gene (22). However, the mode of action of procaine and procainamide probably relies on their intercalation into GC-rich DNA, which seemed to be contradictory to the reported specificity of procainamide (20, 38–40).

Our study establishes nanaomycin A as a novel DNMT inhibitor. The biochemical *in vitro* methylation assays support the finding that DNMT3B is the major DNMT target of nanaomycin A. Molecular docking studies of nanaomycin A using a homology model of the catalytic domain of DNMT3B suggest that an extensive hydrogen bond network with Glu<sup>697</sup>, Arg<sup>731</sup>, and Arg<sup>733</sup> plays a key role in the stabilization of the protein-ligand complex. Similar interactions were not observed in docking studies of nanaomycin A with DNMT1, and these results may explain, at least in part, the structural basis of selectivity. It should be noted that, in contrast to a knockdown, blocking DNMT3B with a small-molecule inhibitor would abolish DNMT3B function without depleting it from the cellular proteomic pool. This will still permit, for example, protein-protein interactions, which might weaken the consequences of DNMT3B inhibition. Additionally, DNMT3B is also known to be expressed in multiple splice variants in cancer cells with unknown functions (41). Some of them encode truncated DNMT3B proteins, which might also be able to bind nanaomycin A.

Based on the experimental and theoretical evidence of the reaction between quinones and cysteine-rich proteins, and the docking model developed for nanaomycin A, we hypothesize the following mechanism for inhibition of DNMT3B with nanaomycin A. Cys<sup>651</sup>-S<sup>-</sup> initiates

**Figure 5.** A, dose-response plots of nanaomycin A against DNMT1 and DNMT3B. The IC<sub>50</sub> concentrations were determined by biochemical DNMT assays under identical conditions (500 nmol/L DNMT, 0.7 μmol/L AdoMet, and 400 nmol/L hemimethylated oligo). Points, mean of three measurements; bars, SD. The data were analyzed by SigmaPlot version 10.0. B, docking model of nanaomycin A with DNMT3B. Selected amino acid residues of the binding site are shown. Hydrogen bonds are indicated with magenta dashes. Nonpolar hydrogen atoms are omitted for clarity.



a nucleophilic Michael 1,4 addition to the  $\alpha,\beta$ -unsaturated carbonyl system at the  $\beta$  carbon, which proceeds on the less steric side (Supplementary Fig. S1). Noteworthy, in the docking model, the sulfur atom of Cys<sup>651</sup> is close to the  $\beta$  carbon. The diene pushes its electron toward the opposite carbonyl atom. Subsequently, an intermediate enolate forms at the carbonyl atom (C-11) and the oxygen atom (O-10; Supplementary Fig. S1). This occurs as a result of the resonance between the delocalization of the anionic charge of the oxygen and the carbonyl atoms. However, the enol isoform of nanaomycin A structure does result; the negative charge located on the oxygen is further stabilized by interaction with positive residues Arg<sup>731</sup> and Arg<sup>733</sup>. This stabilization, plus the covalent addition of the thiol group (Cys<sup>651</sup>-S<sup>-</sup>), blocks the catalytic site DNMT3B. Our binding model of DNMT3B with nanaomycin A is compatible with the described 1,4-addition mechanism. Interestingly, this stabilization is not favored in DNMT1, which has a larger binding pocket. Thus, the selectivity of nanaomycin A toward DNMT3B is probably due to a better stability in the catalytic domain.

The findings of the biochemical assay and the *in silico* modeling data are supported by the results of the *in vivo* experiments. Treatment of different cell lines with nanaomycin A showed a significant genomic demethylation, although, as expected, at a lower level than observed for the nonselective DNMT inhibitor 5-azacytidine. Similar findings were reported for mouse embryonic fibroblasts, where constitutive or conditional deletion of Dnmt3b resulted in genomic demethylation of endogenous C-type retroviral DNA. These results have suggested that Dnmt3b, in addition to the major maintenance methyltransferase Dnmt1, is required for maintaining DNA methylation in these cells (42). Although the level of demethylation at the *RASSF1A* promoter region remained

lower than that of the genome, it was still sufficient to re-activate transcription and expression of this gene and was comparable with the effects observed with other nonnucleoside inhibitors (20, 22). This result is also in agreement with the data obtained from antisense oligonucleotide-mediated knockdown of DNMT3B in A549 cells (33), inducing antiproliferative effects as well as a similar limited *RASSF1A* promoter demethylation associated with reactivated transcription.

Although it is debatable whether the anthracycline group is a good candidate for clinical drug testing due to some lasting cardiotoxicity issues (43), nanaomycin A represents the first non-SAH DNMT3B-selective compound and provides a valuable biochemical tool and benchmark for future studies.

### Disclosure of Potential Conflicts of Interest

No potential conflicts of interest were disclosed.

### Acknowledgments

We thank the Drug Synthesis and Chemistry Branch, NCI, for providing nanaomycin A, and Andre Leischwitz and Berit Haldemann from the German Cancer Research Center core facility for their support.

### Grant Support

This work was supported in part by the State of Florida, Executive Office of the Governor's Office of Tourism, Trade, and Economic Development. J.L.M.-F. thanks the Menopause & Women's Health Research Center for funding.

The costs of publication of this article were defrayed in part by the payment of page charges. This article must therefore be hereby marked *advertisement* in accordance with 18 U.S.C. Section 1734 solely to indicate this fact.

Received 06/30/2010; revised 09/01/2010; accepted 09/07/2010; published OnlineFirst 09/10/2010.

### References

- Campos EI, Reinberg D. Histones: annotating chromatin. *Annu Rev Genet* 2009;43:559–99.
- Cheng X, Blumenthal RM. Coordinated chromatin control: structural and functional linkage of DNA and histone methylation. *Biochemistry* 2010;49:2999–3008.
- Bestor TH. The DNA methyltransferases of mammals. *Hum Mol Genet* 2000;9:2395–402.
- Chen T, Hevi S, Gay F, et al. Complete inactivation of DNMT1 leads to mitotic catastrophe in human cancer cells. *Nat Genet* 2007;39:391–6.
- Goll MG, Bestor TH. Eukaryotic cytosine methyltransferases. *Annu Rev Biochem* 2005;74:481–514.
- Okano M, Bell DW, Haber DA, Li E. DNA methyltransferases Dnmt3a and Dnmt3b are essential for *de novo* methylation and mammalian development. *Cell* 1999;99:247–57.
- Esteller M. Cancer epigenomics: DNA methylomes and histone-modification maps. *Nat Rev Genet* 2007;8:286–98.
- Lyko F, Brown R. DNA methyltransferase inhibitors and the development of epigenetic cancer therapies. *J Natl Cancer Inst* 2005;97:1498–506.
- Suzuki M, Sunaga N, Shames DS, Toyooka S, Gazdar AF, Minna JD. RNA interference-mediated knockdown of DNA methyltransferase 1 leads to promoter demethylation and gene re-expression in human lung and breast cancer cells. *Cancer Res* 2004;64:3137–43.
- Brueckner B, Kuck D, Lyko F. DNA methyltransferase inhibitors for cancer therapy. *Cancer J* 2007;13:17–22.
- Brueckner B, Garcia Boy R, Siedlecki P, et al. Epigenetic reactivation of tumor suppressor genes by a novel small-molecule inhibitor of human DNA methyltransferases. *Cancer Res* 2005;65:6305–11.
- Schirmacher E, Beck C, Brueckner B, et al. Synthesis and *in vitro* evaluation of biotinylated RG108: a high affinity compound for studying binding interactions with human DNA methyltransferases. *Bioconjug Chem* 2006;17:261–6.
- Stresemann C, Brueckner B, Musch T, Stopper H, Lyko F. Functional diversity of DNA methyltransferase inhibitors in human cancer cell lines. *Cancer Res* 2006;66:2794–800.
- Gao Z, Xu Z, Hung MS, et al. Promoter demethylation of WIF-1 by epigallocatechin-3-gallate in lung cancer cells. *Anticancer Res* 2009;29:2025–30.
- Fang MZ, Wang Y, Ai N, et al. Tea polyphenol (–)-epigallocatechin-3-gallate inhibits DNA methyltransferase and reactivates methylation-silenced genes in cancer cell lines. *Cancer Res* 2003;63:7563–70.
- Lee WJ, Zhu BT. Inhibition of DNA methylation by caffeic acid and



- chlorogenic acid, two common catechol-containing coffee polyphenols. *Carcinogenesis* 2006;27:269–77.
17. Kuck D, Singh N, Lyko F, Medina-Franco JL. Novel and selective DNA methyltransferase inhibitors: docking-based virtual screening and experimental evaluation. *Bioorg Med Chem* 2010;18:822–9.
  18. Segura-Pacheco B, Perez-Cardenas E, Taja-Chayeb L, et al. Global DNA hypermethylation-associated cancer chemotherapy resistance and its reversion with the demethylating agent hydralazine. *J Transl Med* 2006;4:32.
  19. Arce C, Segura-Pacheco B, Perez-Cardenas E, Taja-Chayeb L, Candelaria M, Duennas-Gonzalez A. Hydralazine target: from blood vessels to the epigenome. *J Transl Med* 2006;4:10.
  20. Villar-Garea A, Fraga MF, Espada J, Esteller M. Procaine is a DNA-demethylating agent with growth-inhibitory effects in human cancer cells. *Cancer Res* 2003;63:4984–9.
  21. Castellano S, Kuck D, Sala M, Novellino E, Lyko F, Sbardella G. Constrained analogues of procaine as novel small molecule inhibitors of DNA methyltransferase-1. *J Med Chem* 2008;51:2321–5.
  22. Lee BH, Yegnasubramanian S, Lin X, Nelson WG. Procainamide is a specific inhibitor of DNA methyltransferase 1. *J Biol Chem* 2005;280:40749–56.
  23. Lin RK, Hsu CH, Wang YC. Mithramycin A inhibits DNA methyltransferase and metastasis potential of lung cancer cells. *Anticancer Drugs* 2007;18:1157–64.
  24. Suzuki T, Miyata N. Epigenetic control using natural products and synthetic molecules. *Curr Med Chem* 2006;13:935–58.
  25. Yu N, Wang M. Anticancer drug discovery targeting DNA hypermethylation. *Curr Med Chem* 2008;15:1350–75.
  26. Bouma J, Beijnen JH, Bult A, Underberg WJ. Anthracycline antitumor agents. A review of physicochemical, analytical and stability properties. *Pharm Weekbl Sci* 1986;8:109–33.
  27. Galm U, Hager MH, Van Lanen SG, Ju J, Thorson JS, Shen B. Antitumor antibiotics: bleomycin, enediyne, and mitomycin. *Chem Rev* 2005;105:739–58.
  28. Tanaka H, Marumo H, Nagai T, Okada M, Taniguchi K. Nanaomycins, new antibiotics produced by a strain of *Streptomyces*. III. A new component, nanaomycin C, biological activities of nanaomycin derivatives. *J Antibiot (Tokyo)* 1975;28:925–30.
  29. Marumo H, Kitaura K, Morimoto M, Tanaka H, Omura S. The mode of action of nanaomycin A in Gram-positive bacteria. *J Antibiot (Tokyo)* 1980;33:885–90.
  30. Hayashi M, Unemoto T, Minami-Kakinuma S, Tanaka H, Omura S. The mode of action of nanaomycins D and A on a gram-negative marine bacterium *Vibrio alginolyticus*. *J Antibiot (Tokyo)* 1982;35:1078–85.
  31. Stach D, Schmitz OJ, Stilgenbauer S, et al. Capillary electrophoretic analysis of genomic DNA methylation levels. *Nucleic Acids Res* 2003;31:E2.
  32. Siedlecki P, Garcia Boy R, Comagic S, et al. Establishment and functional validation of a structural homology model for human DNA methyltransferase 1. *Biochem Biophys Res Commun* 2003;306:558–63.
  33. Beaulieu N, Morin S, Chute IC, Robert MF, Nguyen H, MacLeod AR. An essential role for DNA methyltransferase DNMT3B in cancer cell survival. *J Biol Chem* 2002;277:28176–81.
  34. Isakovic L, Saavedra OM, Llewellyn DB, et al. Constrained (L)-S-adenosyl-L-homocysteine (SAH) analogues as DNA methyltransferase inhibitors. *Bioorg Med Chem Lett* 2009;19:2742–6.
  35. Saavedra OM, Isakovic L, Llewellyn DB, et al. SAR around (L)-S-adenosyl-L-homocysteine, an inhibitor of human DNA methyltransferase (DNMT) enzymes. *Bioorg Med Chem Lett* 2009;19:2747–51.
  36. Jia D, Jurkowska RZ, Zhang X, Jeltsch A, Cheng X. Structure of Dnmt3a bound to Dnmt3L suggests a model for *de novo* DNA methylation. *Nature* 2007;449:248–51.
  37. Chuang JC, Yoo CB, Kwan JM, et al. Comparison of biological effects of non-nucleoside DNA methylation inhibitors versus 5-aza-2'-deoxycytidine. *Mol Cancer Ther* 2005;4:1515–20.
  38. Campbell VW, Davin D, Thomas S, et al. The G-C specific DNA binding drug, mithramycin, selectively inhibits transcription of the C-MYC and C-HA-RAS genes in regenerating liver. *Am J Med Sci* 1994;307:167–72.
  39. Miller DM, Polansky DA, Thomas SD, et al. Mithramycin selectively inhibits transcription of G-C containing DNA. *Am J Med Sci* 1987;294:388–94.
  40. Yokochi T, Robertson KD. Doxorubicin inhibits DNMT1, resulting in conditional apoptosis. *Mol Pharmacol* 2004;66:1415–20.
  41. Ostler KR, Davis EM, Payne SL, et al. Cancer cells express aberrant DNMT3B transcripts encoding truncated proteins. *Oncogene* 2007;26:5553–63.
  42. Dodge JE, Okano M, Dick F, et al. Inactivation of Dnmt3b in mouse embryonic fibroblasts results in DNA hypomethylation, chromosomal instability, and spontaneous immortalization. *J Biol Chem* 2005;280:17986–91.
  43. Horenstein MS, Vander Heide RS, L'Ecuyer TJ. Molecular basis of anthracycline-induced cardiotoxicity and its prevention. *Mol Genet Metab* 2000;71:436–44.

# Molecular Cancer Therapeutics

## Nanaomycin A Selectively Inhibits DNMT3B and Reactivates Silenced Tumor Suppressor Genes in Human Cancer Cells

Dirk Kuck, Thomas Caulfield, Frank Lyko, et al.

*Mol Cancer Ther* 2010;9:3015-3023. Published OnlineFirst September 10, 2010.

**Updated version** Access the most recent version of this article at:  
doi:[10.1158/1535-7163.MCT-10-0609](https://doi.org/10.1158/1535-7163.MCT-10-0609)

**Supplementary Material** Access the most recent supplemental material at:  
<http://mct.aacrjournals.org/content/suppl/2010/09/10/1535-7163.MCT-10-0609.DC1>  
<http://mct.aacrjournals.org/content/suppl/2010/11/05/1535-7163.MCT-10-0609.DC2>

**Cited articles** This article cites 43 articles, 11 of which you can access for free at:  
<http://mct.aacrjournals.org/content/9/11/3015.full#ref-list-1>

**Citing articles** This article has been cited by 6 HighWire-hosted articles. Access the articles at:  
<http://mct.aacrjournals.org/content/9/11/3015.full#related-urls>

**E-mail alerts** [Sign up to receive free email-alerts](#) related to this article or journal.

**Reprints and Subscriptions** To order reprints of this article or to subscribe to the journal, contact the AACR Publications Department at [pubs@aacr.org](mailto:pubs@aacr.org).

**Permissions** To request permission to re-use all or part of this article, use this link  
<http://mct.aacrjournals.org/content/9/11/3015>.  
Click on "Request Permissions" which will take you to the Copyright Clearance Center's (CCC) Rightslink site.